Article

Hydrometallurgical Extraction of Li and Co from LiCoO$_2$ Particles–Experimental and Modeling

Maria del Mar Cerrillo-Gonzalez[ID]**, Maria Villen-Guzman ***[ID]**, Luis Fernando Acedo-Bueno, Jose Miguel Rodriguez-Maroto**[ID] **and Juan Manuel Paz-Garcia**[ID]

Department of Chemical Engineering, University of Malaga, 29010 Malaga, Spain; mcerrillog@uma.es (M.d.M.C.-G.); luisfernandoacedo@uma.es (L.F.A.-B.); maroto@uma.es (J.M.R.-M.); juanma.paz@uma.es (J.M.P.-G.)
* Correspondence: mvillen@uma.es

check for updates

Featured Application: The physicochemical model described in this work will be useful for the optimization of hydrometallurgical and combined electrochemical–hydrometallurgical recycling processes for spent lithium-ion batteries.

Abstract: The use of lithium-ion batteries as energy storage in portable electronics and electric vehicles is increasing rapidly, which involves the consequent increase of battery waste. Hence, the development of reusing and recycling techniques is important to minimize the environmental impact of these residues and favor the circular economy goal. This paper presents experimental and modeling results for the hydrometallurgical treatment for recycling LiCoO$_2$ cathodes from lithium-ion batteries. Previous experimental results for hydrometallurgical extraction showed that acidic leaching of LiCoO$_2$ particles produced a non-stoichiometric extraction of lithium and cobalt. Furthermore, the maximum lithium extraction obtained experimentally seemed to be limited, reaching values of approximately 65–70%. In this paper, a physicochemical model is presented aiming to increase the understanding of the leaching process and the aforementioned limitations. The model describes the heterogeneous solid–liquid extraction mechanism and kinetics of LiCoO$_2$ particles under a weakly reducing environment. The model presented here sets the basis for a more general theoretical framework that would describe the process under different acidic and reducing conditions. The model is validated with two sets of experiments at different conditions of acid concentration (0.1 and 2.5 M HCl) and solid to liquid ratio (5 and 50 g L^{-1}). The COMSOL Multiphysics program was used to adjust the parameters in the kinetic model with the experimental results.

Keywords: battery recycling; COMSOL; unreacted shrinking core model

1. Introduction

In the last three decades, lithium-ion batteries (LIBs) have prevailed over the other types of secondary batteries due to their advantageous properties, such as high energy density or low self-discharge [1]. The growing use of LIBs encourages the development of reusing and recycling techniques aiming to minimize the environmental impact of the LIB technology and to favor the circular economy goal [2,3].

Different technologies for LIBs recycling have been developed [2]. Among them, pyro- and hydrometallurgical methods are the most commonly used today. Biometallurgical and combined bio-electro-pyro-hydrometallurgical methods are also being developed [4–6]. Pyrometallurgical methods are based on the treatment of LIBs at high temperatures to produce pyrolysis, metal reduction, and subsequent gas incineration. Despite the easiness of the procedure and the optimal technology

readiness, some important drawbacks associated with this method are high energy consumption, hazardous gaseous emissions, loss of metals (Li) in the slag, high amount of slags, and limited recovery rates of metals [7]. On the other hand, hydrometallurgy recycling processes consist of the recovery of metals via acidic leaching, extraction, and precipitation. Compared to pyrometallurgical methods, hydrometallurgy has higher recovery efficiency, lower energy consumption, and lower gaseous emissions. Hence, hydrometallurgical LIB recycling is gaining attention as a more environmentally friendly approach than pyrometallurgical [8].

In hydrometallurgical methods, it is common to use strong inorganic acids, such as HCl [9], HNO_3 [10], and H_2SO_4 [11,12], as leaching reagents. The use of organic acids is being explored as an alternative to reduce the footprint of recycling processes [13]. Moreover, the addition of reductant agents has been probed to significantly improve leaching efficiency.

The understanding on the interaction between solid waste and extracting solution is essential to optimize the selectivity and extraction efficiency of the metals [14]. For that, the proposal of models to describe solid–liquid heterogeneous interactions is especially useful. Different versions of the shrinking core model (SCM) [15–19] have been proposed to evaluate the kinetics of heterogeneous reactions. The SCM considers that the reaction takes place initially at the outer surface of the solid particle and involves the particle size decreasing as the products are formed. That way, the deeper areas of the solid take part in the reaction as they are exposed to the extracting fluid, which involves the constant movement of the reaction zone. The core and the size of the solid particle decrease during the reaction time until they are entirely consumed. These kinds of heterogeneous models take into account the rate control mechanisms, from surface chemical reaction control, Equation (1), to mass transfer control, Equation (2)

$$t/t^* = 1 - (1-X)^{1/3} \quad ; \quad \text{for chemical reaction control} \tag{1}$$

$$t/t^* = 1 - 3(1-X)^{2/3} + 2(1-X) \quad ; \quad \text{for film diffusion control} \tag{2}$$

where t is time and X is the extraction extent of the target metal.

The unreacted shrinking core model (USCM) takes into account the conversion of the reactant into another solid phase, which accumulates in the outer part of the particles. In this model, the size of the unreacted core decreases but the overall particle size remains approximately constant [20]. Several studies have proposed the USCM to evaluate the leaching kinetics of the metals from [21–23]. From comparison of experimental and theoretical results, Zhang et al. in [15] concluded that these models were not suitable to describe the leaching of metals from the cathode scraps. They also evaluated the kinetics of the leaching processes using the Avrami Equation (3), which was initially proposed to describe crystallization kinetics and to give an indication of the crystal growth process.

$$-\ln(1-X) = kt^n \quad ; \quad \text{for the Avrami model} \tag{3}$$

Although the unreacted shrinking core and the Avrami models can satisfactorily fit the experimental observations, they lack the ability to describe the physicochemical particularities of the process. In particular, from our previous results on Li and Co extraction from $LiCoO_2$ particles via acidic leaching [24], two important observations were pointed out:

1. Li and Co extraction does not happen according to the stoichiometry of 1:1 expected from the dissolution of $LiCoO_2$ particles. More specifically, the molar amount of Li extracted seemed to be twice as much as that of Co.
2. Leaching of $LiCoO_2$ particles does not happen to a full extent in reasonable times. The leaching process slows down to an apparent plateau in around 65–70% of Li extraction.

As mentioned before, to the best of our knowledge, the SCM, USCM, and the Avrami model do not deal properly with the aforementioned limitations (Li:Co extraction in a proportion 2:1 and limiting Li extraction to around 65%). Therefore, a mathematical model is proposed for the leaching kinetics of $LiCoO_2$ particles. The model is described from the stoichiometric reactions reported in the

bibliography and takes into account the formation of an insoluble crust of Co_3O_4, which resembles the USCM. The formation of the Co_3O_4 crust was detected through X-ray photoelectron spectroscopy in [24]. The model is validated with two sets of experiments at different conditions of pH and solid to liquid ratios.

2. Materials and Methods

2.1. Extraction Experiments

The experimental system consists of 50 mL polypropylene screw-cap vials. A certain amount of $LiCoO_2$ powder (97% Alfa Aesar, Kandel, Germany) was put in contact with 25 mL of HCl aqueous solution (HCl, 35%, analytical grade, Panreac, Barcelona, Spain) as indicated in Table 1. The vials were continuously stirred on a rotatory shaker at 200 rpm for different contact times at 25 °C. In order to obtain a transient profile for the study of the leaching rate, different vials with identical initial conditions were used. Those vials were withdrawn at selected different times for analysis. Accordingly, no probe sampling was used during the experimental procedure. Each experiment was carried out by triplicate to assure reproducibility.

Table 1. Experimental parameters.

	m_{LiCoO2} (mg)	$V_{solution}$ (mL)	S/L (g L^{-1})	[HCl] (M)
Experiment A	125	25	5	0.1
Experiment B	1250	25	50	2.5

2.2. Analytics

Withdrawn vials were centrifuged at 3800 rpm for five minutes. The supernatant was separated and filtered using 0.6 microm glass-fiber (Macherey-Nagel (MN) GF-3, Düren, Germany) for Co and Li quantitative analysis via atomic absorption spectrophotometry (Varian SpectrAA 1101, Palo Alto, Santa Clara, CA, USA). The pH values of aqueous solutions from experiment A were measured using a pH meter (Crison, Barcelona, Spain). The proton concentration in experiment B was determined by potentiometric titration adding NaOH (Sigma Aldrich, Darmstadt, Germany) solution, assuring pH values below 3 to avoid metal precipitation. The total content of metals was determined by microwave-assisted acid digestion following the guidelines of the EPA method 3051A: A representative dry solid sample of up to 100 mg was extracted and dissolved in 6 mL concentrated nitric acid and 9 mL concentrated hydrochloric acid.

2.3. Physicochemical Model

The dissolution reaction of $LiCoO_2$ particles in acid media, expressed as a redox half-reaction, can be described as [25]:
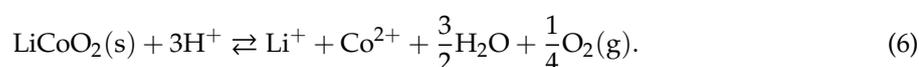
$$LiCoO_2(s) + 4H^+ + e^- \rightleftarrows Li^+ + Co^{2+} + 2H_2O, \tag{4}$$
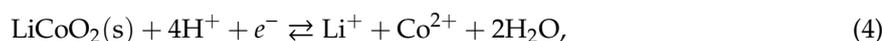
where Co^{3+} within the $LiCoO_2$ particle is reduced to soluble Co^{2+}.

Considering that water acts as the reducing agent of the Co^{3+} as

$$O_2(g) + 4H^+ + 4e^- \rightleftarrows 2H_2O, \tag{5}$$

the redox pair that describes the $LiCoO_2$ particles' dissolution can be expressed as:

$$LiCoO_2(s) + 3H^+ \rightleftarrows Li^+ + Co^{2+} + \frac{3}{2}H_2O + \frac{1}{4}O_2(g). \tag{6}$$

As mentioned before, it was experimentally observed that the amount of extracted Li was nearly twice as much as that of Co, and that, in the absence of stronger reducing agents, the reaction reaches a maximum near 65–70% of Li extraction. A possible explanation for this phenomenon is the formation of a crust of insoluble $Co_3O_4(s)$ according to:

$$LiCoO_2(s) + H^+ \rightleftarrows Li^+ + \frac{1}{3}Co_3O_4(s) + \frac{1}{2}H_2O + \frac{1}{12}O_2(g). \tag{7}$$
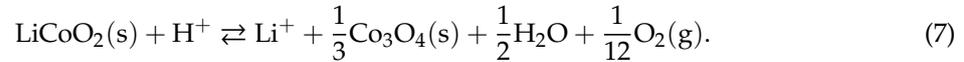
As the Co_3O_4 is insoluble even in concentrated acid, it is likely to form a crust in the particle that will impose resistance to the diffusion of the reactants, H^+ in this case, and could eventually stop the reaction [26]. Accordingly, the model presented here is a variation of the unreacted shrinking core model, and it is depicted in Figure 1.
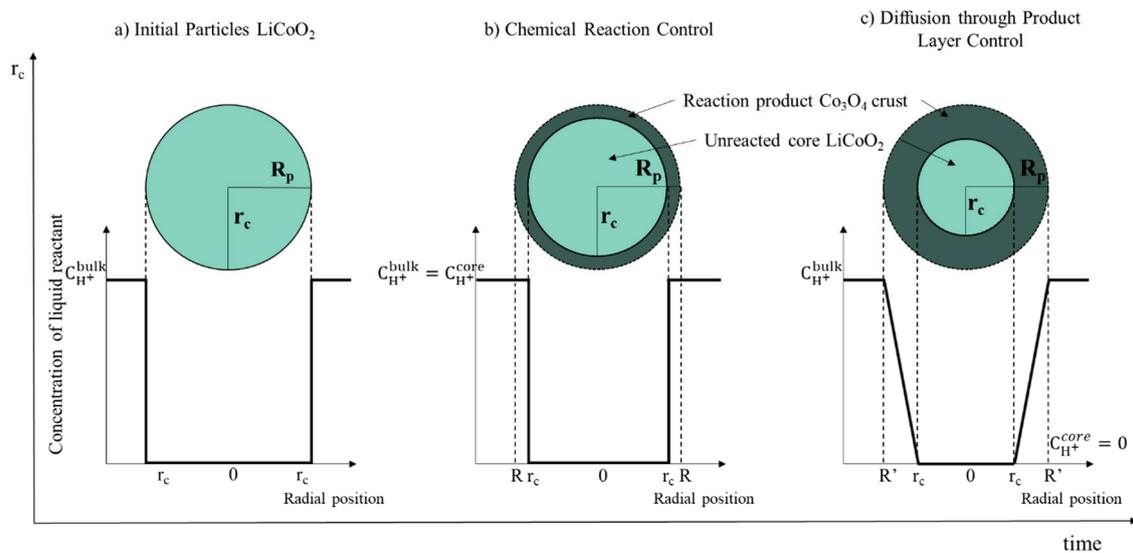

Figure 1. Time transition of the radius core $LiCoO_2$ particles. (**a**) Initial particles. (**b**) Process rate controlled by the chemical kinetics. (**c**) Process rate controlled by the diffusion through the outer layer.

The model is based on the following assumptions:

1. $LiCoO_2$ particles are assumed to be spherical with a mean initial radius of $R_p = 5$ µm that follows a normal distribution. During the reaction, the radius of the unreacted core decreases while the number of particles is considered constant.

2. The extraction of lithium and cobalt from $LiCoO_2$ particles in acidic aqueous solution takes place according to the stoichiometry in Equation (8), which takes into account that the dissolution of $LiCoO_2$ particles produces Li and Co in a proportion of 2:1, as well as the formation of an outer crust layer of $Co_3O_4(s)$ in the external surface of $LiCoO_2(s)$ core.

$$LiCoO_2(s) + 2H^+ \rightarrow Li^+ + \frac{1}{2}Co^{2+} + \frac{1}{6}Co_3O_4(s) + H_2O + \frac{1}{6}O_2(g) \tag{8}$$
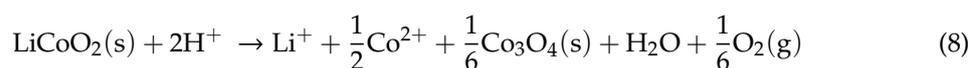
3. The kinetic rate for the reaction in Equation (8) is given by:

$$\frac{dN_{LiCoO_2}}{dt} = \rho_A \, n_p \left(4\pi r_c^2\right)\frac{dr_c}{dt} = -n_p k_r \left(4\pi r_c^2\right)\left(C_{H^+}^{core}\right)^\alpha = -r_{Li^+} \tag{9}$$

where ρ_A (mol m^{-3}) is the molar density of $LiCoO_2$, n_p (–) is the number of particles, r_c (m) is the radius of the unreacted core, k_r (mol$^{1-\alpha}$m$^{3\alpha-2}$s^{-1}) is the kinetic constant and $C_{H^+}^{core}$ (mol m^{-3}) is the concentration of protons in the position r_c, and α (–) is the reaction order with respect to the protons.

4. The rate of Li^+ and Co^{2+} production and H^+ consumption in the extracting liquid, assumed with a constant volume of V_L (m³), is given by:

$$V_L \frac{dC_{Li^+}}{dt} = r_{Li^+} \tag{10}$$

$$V_L \frac{dC_{Co^{2+}}}{dt} = \frac{1}{2} r_{Li^+} \tag{11}$$

$$V_L \frac{dC_{H^+}}{dt} = -2 r_{Li^+} \tag{12}$$

5. The outer crust of Co_3O_4 (s), which forms during the process, is supposed to be porous. As it forms, the size of the particle remains constant and equal to the initial. Diffusion of the reactant, namely, the H^+, through the layer of $Co_3O_4(s)$ from the bulk liquid to the surface of the unreacted core is described as:

$$V_L \frac{dC_{H^+}}{dt} = -\frac{D_{H^+}^{\mathrm{eff}} \left(C_{H^+}^{bulk} - C_{H^+}^{core} \right)}{\left(R_p - r_c \right)} n_p \left(4\pi R_p r_c \right) \tag{13}$$

where $C_{H^+}^{bulk}$ is the concentration of protons in the bulk liquid, and $D_{H^+}^{\mathrm{eff}}$ (m² s⁻¹) is the effective diffusion coefficient of the proton through the layer of Co_3O_4. The effective diffusion coefficient is considered to change as the crust increases, according to the following expression:

$$D_{H^+}^{\mathrm{eff}} = D_{H^+} \, \epsilon \exp \left(k_D X_{Co} \left(R_p - r_c \right) \right). \tag{14}$$

D_{H^+} (m² s⁻¹) is the diffusion coefficient at infinite dilution (9.311×10^{-9} m² s⁻¹ [27]), ϵ (–) is the porosity, X_{Co} (–) is the percentage of cobalt extracted, and k_D (m⁻¹) is a parameter that measures the increase of the resistance to the mass transport as the crust increases as a consequence of changes in porosity or tortuosity, including pore closing due to counter diffusion of the O_2 gas formed in the reaction. X_{Co} (–) is included in the equation to take into account the formation of O_2 (g) and accumulation within the porous structure.

6. As the reaction proceeds and the outer $Co_3O_4(s)$ crust increases, resistance to the diffusion transport increases according to Equation (14). At a certain thickness of the crust, the process reaches a point in which the rate of proton diffusion is lower than the chemical kinetic consumption. At this point, as soon as protons reach the reactive surface, they are consumed by the reaction. The second Damköhler number, Da_{II} (–), defined in Equation (15) as the ratio of the chemical reaction rate to the mass transfer rate, is used to identify the controlling mechanisms.

$$Da_{II} = \frac{\text{kinetics rate}}{\text{diffussion rate}} = \frac{k_r}{D_H^{\mathrm{eff}}} \left(C_{H^+}^{core} \right)^\alpha \left(R_p - r_c \right). \tag{15}$$

7. Combining Equations (9), (12), and (13), it can stated that:

$$-2 r_{Li^+} = -\frac{D_{H^+}^{\mathrm{eff}} \left(C_{H^+}^{bulk} - C_{H^+}^{core} \right)}{\left(R_p - r_c \right)} n_p (4\pi R r_c) - 2 n_p k \left(4\pi r_c^2 \right) \left(C_{H^+}^{core} \right)^\alpha \tag{16}$$

where, if $Da_{II} \leq 1$, then $C_{H^+}^{core} = C_{H^+}^{bulk}$, and the process rate is defined by the chemical kinetics law. However, whenever $Da_{II} > 1$, then $C_{H^+}^{core} = 0$, and the process rate is controlled by the diffusion. The change of control mechanism is schematized in Figure 1.

8. The Diffusion of Li^+ and Co^{2+} through the $Co_3O_4(s)$ crust layer to the bulk solution is considered to have no effect on the process rate. Additionally, the system is considered well stirred to assume

　　the mass transfer resistance through the limit layer between the bulk solution and the solid
　　surface is negligible.

3. Results and Discussion

　　In this section, the experimental and simulation results are presented and discussed for the two
experimental cases. The parameters used for the simulations are listed in Table 2. The software
COMSOL Multiphysics 5.5 was used for the numerical integration of the partial differential equations
describing the dissolution of $LiCoO_2$ particles and for the parameter optimization.

Table 2. Parameters used in the simulation results.

Parameter	Value (Case A)	Value (Case B)	Unit	Description
k_r	8×10^{-10}	6×10^{-10}	$mol^{-0.5} m\ s^{-1}$	Kinetic constant
k_D	-5.2×10^7	-4.1×10^7	m^{-1}	Diffusion resistance factor
α		3/2	(–)	Order of reaction for H^+

　　Figure 2 shows the percentage of extracted Co and Li (mol/mol%) based on the initial total amount
of Co and Li in the solid for Experiment A (the extraction experiment with S/L = 5 g/L in 0.1 M HCl).
The extracted Co and Li correspond to the Co^{2+} and Li^+ in the solution. According to the results,
the extraction is very fast in the first hours, with a nearly lineal tendency. Then, the extraction rate
decreases, and it becomes asymptotically stabilized. This behavior is consistent with the described
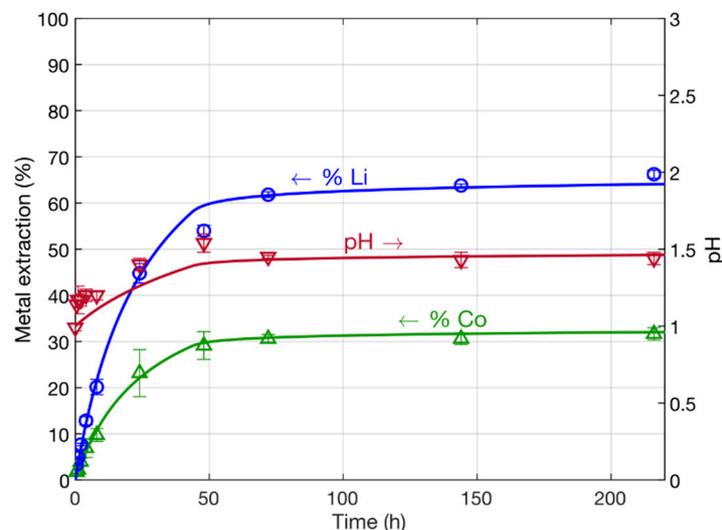switch in the rate controlling mechanisms.

Figure 2. Experimental (marks) and simulation (lines) results for the case of $S/L = 5$ g/L in 0.1 M HCl.

　　As observed before, the extraction of Li is approximately twice as much as that of Co, and the
maximum extracted Li is around 65%. The pH evolution has a similar tendency: Protons are consumed
during the first hours of extraction. After approximately 50 h, the pH stabilizes to a value of pH ≈ 1.5.
This also indicates that the reaction was not stopped due to depletion of protons but for an increase on
the resistance to the mass transport.

　　The simulation results are also presented in Figure 2 in order to be compared with the experimental
data. It can be observed that the simulation results match fairly well with the experimental observations.
The presented model predicts the switch of process rate control as the resistance of the diffusion of
protons increases with the thickness of the crust. To better understand the change of the controlling
mechanisms, in Figure 3a, the calculated Damköhler number for the simulation related to Experiment
A is presented. It can be observed that the reaction rate changes from kinetic to diffusion control

($Da_{II} = 1$) at approximately 50 h. Figure 3b shows the simulation results on the radius decrease of the unreacted core. This value is used to calculate the increase of the resistance modelled in Equation (14), as a consequence of the increase of the thickness of the outer crust.
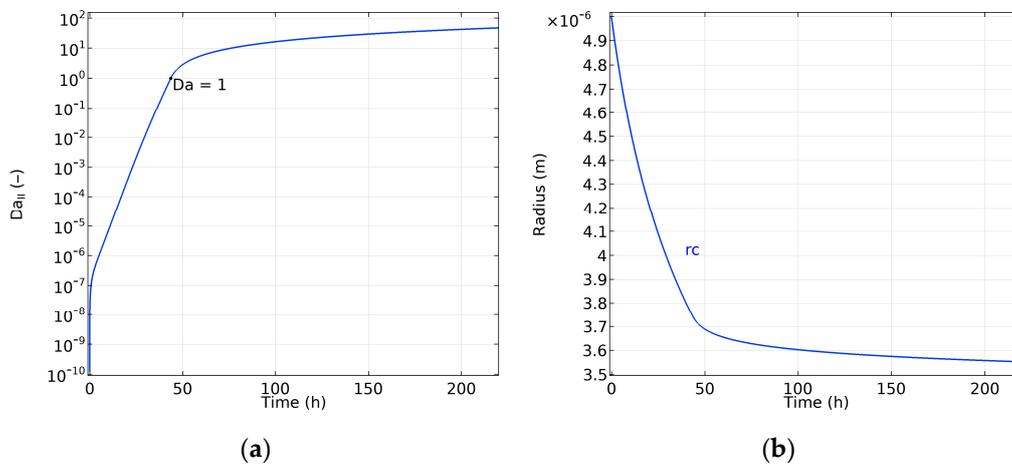

(**a**)　　　　　　　　　　　　　　　　　　　(**b**)

Figure 3. (**a**) Da $_{II}$ for Experiment at HCl 0.1 M and S/L 5 g/L. (**b**) Radius of the particle and the inner core.

Figure 4 shows the experimental and simulation results for the experiment with $S/L = 50$ in 2.5 M HCl. In this case, proton concentration is presented instead of pH due to the high concentration of protons, producing negative pH values. It can be observed that in experiment B, with 10 times higher solid to liquid ratio and 25 times higher acid concentration than in experiment A, asymptotic stabilization occurs much faster. Experiment B reaches asymptotic stabilization in approximately 25 min. However, despite the faster behavior, the same features are observed in these conditions: The maximum Li recovery is near 70%, and the amount of Li extracted is twice as much as that of Co.
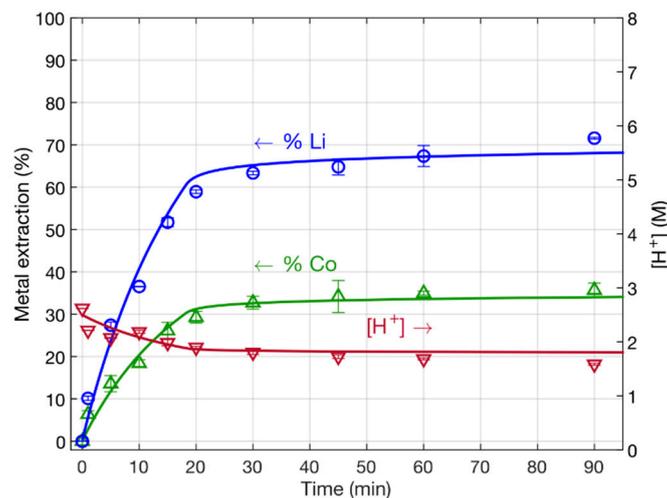

Figure 4. Experimental (marks) and simulation (lines) results for $S/L = 50$ g/L in 2.5 M HCl.

The Li%, Co%, and proton concentration profiles obtained in the simulations presented in Figure 4 were obtained with the parameters listed in Table 2, case B. These values are very similar to those obtained for experiment A. There is a slight variation on the most suitable value for the kinetic constant, which can be attributed to small temperature differences between the experiments. There is also a small variation on the most suitable value for the diffusive resistance factor, which can be linked to the possible deviation due to chemical activity. As the second experiment is carried out in a concentrated solution, the deviation of the activity factor to the diffusion may play a role not considered in the

model. Despite the small variations, the presented model is able to predict the behavior of the acid leaching of $LiCoO_2$ particles in very different conditions.

4. Conclusions

In this paper, a model has been presented for the extraction of lithium and cobalt from $LiCoO_2$ particles, taking into account the switch in the controlling mechanisms, from chemical kinetics to mass transfer. Two sets of experiments have been carried out to validate the model. The comparison between the experimental observations and the simulations shows that the model for the lithium and cobalt extraction from $LiCoO_2$ particles satisfactorily reproduces the experimental results in different conditions. Moreover, the model can predict the non-equimolar proportion between Li^+ and Co^{2+} extracted and the maximum extraction limitation associated with the formation of a Co_3O_4 crust around the particle's core.

Although the model and experiments carried out in this work were focused on $LiCoO_2$ particles and HCl solution, the model can be extended to other cathodes' chemistry and extracting agents. In future works, it is planned to include in this model the effect of using a reducing agent and temperature during the leaching process with the aim to optimize the leaching parameters involved in the hydrometallurgical recycling processes.

References

1. Choubey, P.K.; Chung, K.S.; Kim, M.S.; Lee, J.C.; Srivastava, R.R. Advance review on the exploitation of the prominent energy-storage element Lithium. Part II: From sea water and spent lithium ion batteries (LIBs). *Miner. Eng.* **2017**, *110*, 104–121. [CrossRef]

2. Mossali, E.; Picone, N.; Gentilini, L.; Rodrìguez, O.; Pérez, J.M.; Colledani, M. Lithium-ion batteries towards circular economy: A literature review of opportunities and issues of recycling treatments. *J. Environ. Manag.* **2020**, *264*, 110500. [CrossRef] [PubMed]

3. Wang, Y.; An, N.; Wen, L.; Wang, L.; Jiang, X.; Hou, F.; Yin, Y.; Liang, J. Recent progress on the recycling technology of Li-ion batteries. *J. Energy Chem.* **2020**, *55*, 391–419. [CrossRef]

4. Huang, T.; Liu, L.; Zhang, S. Recovery of cobalt, lithium, and manganese from the cathode active materials of spent lithium-ion batteries in a bio-electro-hydrometallurgical process. *Hydrometallurgy* **2019**, *188*, 101–111. [CrossRef]

5. Sonoc, A.C.; Jeswiet, J.; Murayama, N.; Shibata, J. A study of the application of Donnan dialysis to the recycling of lithium ion batteries. *Hydrometallurgy* **2018**, *175*, 133–143. [CrossRef]

6. Villen-Guzman, M.; Arhoun, B.; Vereda-Alonso, C.; Gomez-Lahoz, C.; Rodriguez-Maroto, J.M.; Paz-Garcia, J.M. Electrodialytic processes in solid matrices. New insights into battery recycling. A review. *J. Chem. Technol. Biotechnol.* **2019**, *94*, 1727–1738. [CrossRef]

7. Georgi-Maschler, T.; Friedrich, B.; Weyhe, R.; Heegn, H.; Rutz, M. Development of a recycling process for Li-ion batteries. *J. Power Sources* **2012**, *207*, 173–182. [CrossRef]

8. Nayaka, G.P.; Manjanna, J.; Pai, K.V.; Vadavi, R.; Keny, S.J.; Tripathi, V.S. Recovery of valuable metal ions from the spent lithium-ion battery using aqueous mixture of mild organic acids as alternative to mineral acids. *Hydrometallurgy* **2015**, *151*, 73–77. [CrossRef]

9. Jha, M.K.; Kumari, A.; Jha, A.K.; Kumar, V.; Hait, J.; Pandey, B.D. Recovery of lithium and cobalt from waste lithium ion batteries of mobile phone. *Waste Manag.* **2013**, *33*, 1890–1897. [CrossRef]

10. Lee, C.K.; Rhee, K.I. Preparation of $LiCoO_2$ from spent lithium-ion batteries. *J. Power Sources* **2002**, *109*, 17–21. [CrossRef]

11. Meshram, P.; Pandey, B.D.; Mankhand, T.R. Hydrometallurgical processing of spent lithium ion batteries (LIBs) in the presence of a reducing agent with emphasis on kinetics of leaching. *Chem. Eng. J.* **2015**, *281*, 418–427. [CrossRef]

12. Li, J.; Yang, X.; Fu, Y.; Huang, H.; Zhong, Z.; Wang, Y. Recovery of Fe, Mn, Ni and Co in sulfuric acid leaching liquor of spent lithium ion batteries for synthesis of lithium ion-sieve and NixCoyMn1-x-y(OH)2. *Hydrometallurgy* **2019**, *190*, 105190. [CrossRef]

13. Musariri, B.; Akdogan, G.; Dorfling, C.; Bradshaw, S. Evaluating organic acids as alternative leaching reagents for metal recovery from lithium ion batteries. *Miner. Eng.* **2019**, *137*, 108–117. [CrossRef]

14. Gao, W.; Liu, C.; Cao, H.; Zheng, X.; Lin, X.; Wang, H.; Zhang, Y.; Sun, Z. Comprehensive evaluation on effective leaching of critical metals from spent lithium-ion batteries. *Waste Manag.* **2018**, *75*, 477–485. [CrossRef]

15. Zhang, X.; Cao, H.; Xie, Y.; Ning, P.; An, H.; You, H.; Nawaz, F. A closed-loop process for recycling LiNi1/3Co1/3Mn1/3O2 from the cathode scraps of lithium-ion batteries: Process optimization and kinetics analysis. *Sep. Purif. Technol.* **2015**, *150*, 186–195. [CrossRef]

16. Ferrier, R.J.; Cai, L.; Lin, Q.; Gorman, G.J.; Neethling, S.J. Models for apparent reaction kinetics in heap leaching: A new semi-empirical approach and its comparison to shrinking core and other particle-scale models. *Hydrometallurgy* **2016**, *166*, 22–33. [CrossRef]

17. Levenspiel, O. Chemical reaction engineering. *Ind. Eng. Chem. Res.* **1999**, *38*, 4140–4143. [CrossRef]

18. Safari, V.; Arzpeyma, G.; Rashchi, F.; Mostoufi, N. A shrinking particle-shrinking core model for leaching of a zinc ore containing silica. *Int. J. Miner. Process.* **2009**, *93*, 79–83. [CrossRef]

19. Raschman, P.; Popovič, Ľ.; Fedoročková, A.; Kyslytsyna, M.; Sučik, G. Non-porous shrinking particle model of leaching at low liquid-to-solid ratio. *Hydrometallurgy* **2019**, *190*, 105151. [CrossRef]

20. Homma, S.; Ogata, S.; Koga, J.; Matsumoto, S. Gas-solid reaction model for a shrinking spherical particle with unreacted shrinking core. *Chem. Eng. Sci.* **2005**, *60*, 4971–4980. [CrossRef]

21. Meng, F.; Liu, Q.; Kim, R.; Wang, J.; Liu, G.; Ghahreman, A. Selective recovery of valuable metals from industrial waste lithium-ion batteries using citric acid under reductive conditions: Leaching optimization and kinetic analysis. *Hydrometallurgy* **2020**, *191*, 105160. [CrossRef]

22. Li, L.; Bian, Y.; Zhang, X.; Xue, Q.; Fan, E.; Wu, F.; Chen, R. Economical recycling process for spent lithium-ion batteries and macro- and micro-scale mechanistic study. *J. Power Sources* **2018**, *377*, 70–79. [CrossRef]

23. Setiawan, H.; Petrus, H.T.B.M.; Perdana, I. Reaction kinetics modeling for lithium and cobalt recovery from spent lithium-ion batteries using acetic acid. *Int. J. Miner. Metall. Mater.* **2019**, *26*, 98–107. [CrossRef]

24. Cerrillo-Gonzalez, M.M.; Villen-Guzman, M.; Vereda-Alonso, C.; Gomez-Lahoz, C.; Rodriguez-Maroto, J.M.; Paz-Garcia, J.M. Recovery of Li and Co from LiCoO2 via Hydrometallurgical–Electrodialytic Treatment. *Appl. Sci.* **2020**, *10*, 2367. [CrossRef]

25. Porvali, A.; Chernyaev, A.; Shukla, S.; Lundström, M. Lithium ion battery active material dissolution kinetics in Fe(II)/Fe(III) catalyzed Cu-H2SO4 leaching system. *Sep. Purif. Technol.* **2020**, *236*, 116305. [CrossRef]

26. Li, L.; Bian, Y.; Zhang, X.; Guan, Y.; Fan, E.; Wu, F.; Chen, R. Process for recycling mixed-cathode materials from spent lithium-ion batteries and kinetics of leaching. *Waste Manag.* **2018**, *71*, 362–371. [CrossRef]

27. Vanýsek, P. Equivalent Conductivity of Electrolytes in Aqueous Solution. In *CRC Handbook of Chemistry and Physics*; CRC Press: Boca Raton, FL, USA, 2013; p. 76.